20th IMEKO TC4 International Symposium and
18th International Workshop on ADC Modelling and Testing
Research on Electric and Electronic Measurement for the Economic Upturn
Benevento, Italy, September 15-17, 2014

Laboratory and field Ground Penetrating Radar measurements for buried weapons detection

Elena Pettinelli[1], Elisabetta Mattei[2], Barbara Cosciotti[1], Federico di Paolo[1] and Sebastian Emauel Lauro[1]

[1] *Dipartimento di Matematica e Fisica,Università degli Studi Roma Tre, Via della Vasca Navale, 84, 00146, Roma, Italy, pettinelli@fis.uniroma3.it*
[2] *Dipartimento di Scienze Ecologiche e Biologiche, Università della Tuscia, Largo dell'Università 11 (snc), 01100 Viterbo, Italy*

***Abstract* – In this work we present the results obtained in two different experiments aimed at evaluating the capability of Ground Penetrating Radar to detect buried metal weapons. The first experiment was conducted acquiring radar data on a layer of synthetic sand in which a metal gun was hidden at shallow depth. The second experiment was conducted in the field, collecting radar data in an area where four different objects were buried (at about 30cm) in sandy volcanic soil. The radar survey was performed for different soil water contents (dry and wet conditions). The results show how the capability to detect the targets and define their depth and shape is strongly dependent on the target depth and orientation with respect to the antenna electric field, as well as to the host material dielectric properties.**

I. INTRODUCTION

Ground Penetrating Radar (GPR) technique can be effectively applied to produce an image of buried targets in a host medium, through the detection of the "boundaries" between objects having different impedances [1,2]. The transmitting antenna emits an electromagnetic short impulse (typically a 1 - 10ns wavelet) which is scattered by the electromagnetic discontinuities present in the subsurface and gathered by the receiving antenna. For each antenna position on the ground, GPR measures the time range (two-way travel time) between the antennas and the buried discontinuities as well as amplitude and phase of the scattered signals. The resulting electromagnetic image, usually called radar cross section (or radargram), is similar to ultrasound images generated in diagnostic medicine. As GPR is particularly suited to detect metallic objects buried in natural or artificial materials, in the last few years such geophysical technique has gain attention of the forensic community [3]. In this work we present some results related to laboratory and field experiments aimed at evaluating the capability to detect metallic weapons buried in different environmental conditions, using a high frequency commercial GPR.

II. LABORATORY SETUP AND FIELD TEST SITE

In the laboratory experiment, a fake gun made of iron was buried inside a dielectric box filled with synthetic sand (see Figure 1). The box (placed on two 80-cm high wooden tables) is made of fiberglass (relative permittivity $\varepsilon_r \cong 3$) and is about 150-cm long, 100-cm wide, and 30-cm high (the walls are approximately 1-cm thick). It is filled with silica glass beads having a diameter range 400-800 μm, which simulates a dry low-magnetic sandy soil. The gun was buried in horizontal position (see Figure 1) at about 9±1 cm depth from the surface. Note that a first set of measurements was performed on the gun buried as it is, whereas a second set of measurements was made on the gun closed in a plastic box, positioning the box at 9±1 cm depth from the surface. In the field experiment, four different objects were buried in sandy volcanic soil: a knife, the fake gun used in the lab experiment, an hatchet and the plastic box used in the previous experiment. The targets were positioned at the four corners of a 1x2 m rectangular area (Figure 2 top) an buried at a depth of about 30±3 cm (Figure 2 bottom). Figure 2 (top) also shows the orientation of the targets with respect to the conventional X and Y axes. The radar measurements were performed in dry and wet conditions (see below).

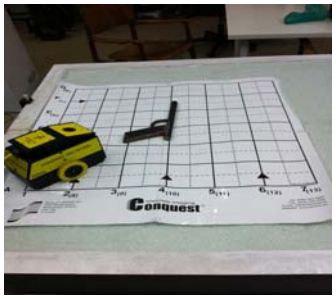

Fig. 1. The metal gun before being buried in the glass beads layer and the 1000MHz antennas used to collect the radar data.

ISBN-14: 978-92-990073-2-7

III. DIELECTRIC PROPERTIES OF HOSTING MATERIALS

The dielectric properties of the materials hosting the targets were measured using Time Domain Reflectivity (TDR) technique. The data were acquired using a three-pronged probe (an open-ended transmission line formed by three stainless-steel parallel rods with a diameter of 0.4 cm, a separating distance of 3.2 cm, and a length of 10 cm). The probe was connected through a 50Ω coaxial line to a Tektronix 1502C cable tester, which applies a step function wave front and measures the signal reflected by the impedance discontinuities. The permittivity was calculated according to equation:

$$\varepsilon = \left(ct/2L\right)^2 \qquad (1)$$

where c is the velocity of light in a vacuum, t is the two-way travel time measured with TDR and L is the length of the probe inserted in the soil. TDR DC conductivity was estimated according to [4]:

$$\sigma_{DC} = \frac{\varepsilon_0^{1/2} Z_0}{\mu_0^{1/2} \cdot L \cdot Z_{coax}} \cdot \left(\frac{2V_0 - V_F}{V_F} \right) \qquad (2)$$

where Z_0 is the feeder transmission line impedance (50 Ω), Z_{coax} is the probe impedance in air, L is its length, V_0 is the TDR input step voltage, and V_F is the final asymptotic voltage (after the reflection process is completely decayed). The dielectric properties of the glass beads used in the lab experiment were measured inserting the probe in several spots inside and outside the area tested with the radar. We found an average permittivity of ε_{gb} = 3.2±0.2, whereas no data have been retrieved on the glass beads DC conductivity as the values were lower than the sensitivity limit of the method. In the field experiment, the hosting material dielectric properties were measured in dry and wet conditions (i.e. after two hours of uniform irrigation of the test site), again inserting the probe in different spots inside and outside the tested area. Table 1 summarizes the permittivity and DC conductivity values collected in the same spots for the dry and wet conditions. The uncertainties were determined from the TDR step rise-time and the geometric features of the line, and were estimated by applying the error linear propagation formula [5].

Table 1.Permittivity values measured with TDR in dry and wet conditions

Position	ε_r(dry)	σ_{DC}(S/m) (dry)	ε_r(wet)	σ_{DC}(S/m) (wet)
P1(dry)	4.5±0.7	(4.41±0.05)x10^{-4}	15.0±1.7	(3.13±0.02)x10^{-3}
P2(dry)	5.5±0.8	(7.63±0.08)x10^{-4}	19.8±2.1	(6.59±0.02)x10^{-3}
P3(dry)	7.5±1.0	(1.49±0.01)x10^{-3}	18.2±2.0	(4.11±0.04)x10^{-3}
P4(dry)	7.8±1.1	(1.70±0.02)x10^{-3}	18.8±2.0	(2.13±0.02)x10^{-3}
P5(dry)	-	-	19.0±2.1	(7.46±0.09)x10^{-3}
P6(dry)	-	-	15.0±1.7	(2.73±0.03)x10^{-3}

IV. GPR MEASUREMENTS

GPR data were collected using a commercial bistatic radar system, the PulseEkko Pro (Sensors and Software) equipped with dipole antennas. In the lab experiment we used the TR1000 MHz, with the dipoles housed in a single case; in the field experiment we used the 500MHz antennas, with the dipoles housed in two different cases. In the laboratory experiment, a 0.6x0.6m area centred above the buried gun was investigated, collecting 13 lines in the X direction and 13 lines in the Y directions, with a line spacing of 5 cm in both directions. The radar lines were acquired with a step size of 0.005m, a trace staking of 4 and a time window of 25 ns. The measurements were performed positioning the antennas on top a 30±1 cm thick layer of glass beads. In the field experiment, both X and Y lines were collected in dry and wet conditions, choosing a line spacing of 10 cm, a step size of 0.01 m, a trace stacking of 4 and a time window of 60 ns.

Subsequently, the radar data were migrated, interpolated and represented in terms of 1 ns thick time slice maps, to illustrate location and shape of the anomaly at different depths.

Fig. 2. Location and orientation of the four targets buried in the soil (top,), and targets burial depth (bottom).

V. RESULTS

Figure 3 (left) shows, as an example, a time slice relevant to the radar data collected on the glass beads when the gun as it is. The slice interpolates the data collected on both X and Y axes. In this clean and homogeneous host material, the gun is clearly detectable and its shape is well recognizable. The anomaly produced by the metal gun starts to become visible at a depth of about 8 cm and extends downward well beyond the real thickness of the gun (about 3cm) to a depth of 18 cm. These depths have been calculated using the permittivity values measured with TDR. Figure 3 (right) also shows

the slice interpolating the radar data collected on both X and Y axes on the buried gun closed into the plastic box. It is interesting to notice that the shape of the anomalies are quite different as, in this case, the gun is located inside an “empty space” and the scattering phenomena are more complex.

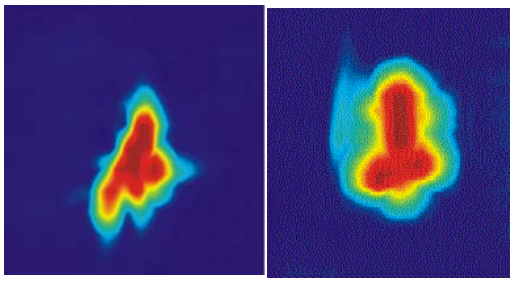

Fig. 3. Radar image of the gun buried in the glass beads .

Figure 4 shows a time slice (1 ns thickness) related to the radar measurements collected in the field test site, along the X axis, in dry conditions. The slice refers to a depth of about 30 cm (time slice 5-6 ns), and illustrates the detection of three anomalies associated to the hatchet, the plastic box and the knife (see Figure 2 for comparison). Conversely to what expected, the metal gun is not detectable in any of the time slices, whereas another anomaly, probably generated by a buried rock, is visible in the lower part of the radar map. Here the two-way travel time has been converted into depth using the average permittivity estimated with TDR in dry conditions. Figure 5 shows a time slice of the radar data collected along the X axis in wet conditions. The time slice (7–8 ns) refers to a depth of about 28 cm, calculated on the basis of the average permittivity estimated with TDR after intense irrigation. In this conditions the best detected target is the plastic box, the knife is still visible but the hatchet has totally “disappeared”. Similar results have been attained for both dry and wet conditions in the data collected along the Y axis (not shown here).

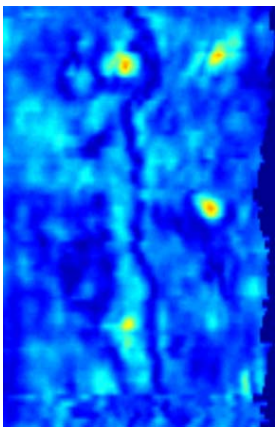

Fig. 4. Radar data collected in dry condition. The time slice only shows the detection of three targets .

VI. CONCLUSIONS

Metal weapons can be well detected if buried at shallow depth in a clean homogeneous host material. In this case, the use of a high frequency radar (1000MHz) also allows to define the shape of the weapon. Moreover, the experiment presented here shows that the radar is capable to detect and recognize the shape and the size of the gun also when this is preserved in a dielectric container (plastic box) and buried at shallow depth.

The validity of these results can be extended to other cases as the high resolution radar images obtained in the glass beads could potentially be recorded in other materials equally transparent to radio waves, like dry non-magnetic sand or dry cement.

On the other hand, the data collected in the field site show that the soil water content and the orientation of the targets with respect to the antenna electric field can strongly affect the capability to find metallic weapons buried at several tens of centimetres. Finally, it is interesting to notice that in wet conditions the shape of the plastic box can be fully determined if the radar data are collected using a interline spacing (≅10cm) comparable to the box dimension.

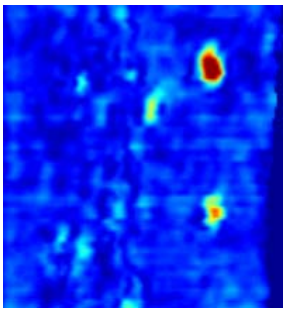

Fig. 1. Radar data collected in wet conditions. After intense irrigation, the radar response is modified and only two targets are clearly recognizable.

ACKNOWLEDGMENTS

The Authors would like to thanks Dr. Pier Matteo Barone and Dr. Carlotta Ferrara for their support in radar data collection.

REFERENCES

[1] A.P. Annan, Ground Penetrating Radar Principles, Procedures & Applications, Sensors & Software Inc., 2004, pp. 180-183.

[2] E. Pettinelli, P.M. Barone, E. Mattei, and S.E. Lauro, 'Radio wave techniques for non-destructive archaeological investigations', Contemporary Physics, 2011, 52: 2, 121 — 130.

[3] A. Ruffell, J. McKinley, Geoforensic, John Wiley & Sons, 2008, pp.340.

[4] K Giese., R Tieman., “Determination of the complex permittivity from thin sample time domain reflectometry: improved analysis of the step response waveform”, Adv. Mol. Relax. Processes, 1975, vol. 7, pp. 45-59.

[5] Evaluation of measurement data — Guide to the expression of uncertainty in measurement - JCGM 100:2008.